Azimuthal angle dependence of optical second harmonic intensity from a vicinal GaAs(001) wafer

Motonari Takebayashi*, Goro Mizutani , and Sukekatsu Ushioda

School of Materials Science, Japan Advanced Institute of Science and Technology, Tatsunokuchi-machi, Nomi-gun, Ishikawa-ken 923-12

(Received

We demonstrate that the tilt angle of a zinc blende type single crystal (001) wafer can be measured by optical second harmonic generation. The SH intensity patterns were analyzed for all four combinations of *p*- and *s*-polarized incidence and output, considering both the bulk and surface optical nonlinearities in the electric dipole approximation. We found that the measurement using *s*-incident polarization is particularly useful in determining the tilt angle of the crystal axes. The parameters determined by the present method agree well with those obtained by X-ray diffraction measurements. The [110] and [$1\bar{1}0$] directions can be distinguished through the analysis of the *p*-incident and *p*-output SH intensity patterns.

PACS codes: 42.65.Ky, 42.65.An, 68.35.Wm, 78.20.Wc

KEYWORDS: optical second harmonic generation, SHG, vicinal GaAs(001), tilt angle, surface nonlinearity

to whom correspondence should be directed at Phone: +81-761-51-1521, Fax: +81-761-51-1149, and E-mail: mizutani@jaist.ac.jp

1. INTRODUCTION

Optical second harmonic generation (SHG) occurs in a medium lacking a center of inversion. It also occurs at surfaces because every surface lacks inversion symmetry. Thus SHG has been used as a tool for investigating surfaces of materials. Recently SHG has been applied to the characterization of wafer substrates of cubic zinc-blende type crystals not only in air but also in vacuum. [1-3] These materials show strong bulk second harmonic responses, because their crystal structures lack inversion symmetry. This bulk SH response is very sensitive to a tilt of the crystal axes and its intensity varies sensitively when surface generated SH signals are also present.[1] It has been pointed out by Bottomley et al that the tilt angle can be determined by analyses of SH intensity patterns [3]. However, they analyzed the SH intensity pattern only for one polarization configuration with *p*-polarized excitation and *s*-polarized output. Furthermore, they did not consider the surface nonlinearity. According to Refs. 1 and 2, it is necessary to consider surface nonlinearity to interpret the SH intensity patterns correctly. In order to consider the surface nonlinearity, the observation of the SH intensity pattern for *p*-polarized excitation and *p*-polarized output is important, because the surface nonlinearity involves excitation of the polarization perpendicular to the surface. The observation for *s*-polarized excitation and *s*-polarized output is also important to pick up the bulk effect independently. Thus, we analyzed all possible polarization combinations, in order to increase the reliability of the analysis. The response for *s*-polarized excitation has never been shown in the literature, perhaps because of its weak signal intensity.

In this paper we have obtained and analyzed the SH intensity patterns of all four polarization combinations of *p*- and *s*-incidence and

output. We chose a GaAs(001) wafer tilted towards the [010] direction as a typical example for demonstration.

2. EXPERIMENT

Figure 1 illustrates the experimental setup for SHG observation. All experiments were performed in air. The system uses a Q-switched Nd:YAG laser operating at 1064nm, 3ns duration, and a repetition rate of 10Hz. The SH signals were detected at 532nm. The laser pulses were passed through a polarizer, a lens, and a visible-cut filter and was focused into a spot of 1mm diameter on the sample surface at an incident angle of 45^{o}. In order to avoid damaging the sample, the incident power was kept below 0.7mJ/pulse. The reflected SH light was passed through an IR-cut filter, a polarizer, lenses, and a monochromator, and was finally detected by a photomultiplier. The output signal from a photomultiplier was accumulated in a personal computer (NEC PC-9801). We corrected for a long-term variation of the laser intensity by monitoring the SH intensity of a reference sample GaAs(100). The system background was 2×10^{-4} photons per laser pulse. The samples were a high-resistivity vicinal GaAs(001) wafer and an n-type GaAs(001) (Si doped) wafer. Their surfaces had a mirror-like finish and were used as delivered without surface treatment. They were mounted on an automatic rotation stage, with the surface normal set parallel to the rotating axis of the stage within an uncertainty of $\pm 0.07^{o}$.

3. THEORETICAL TREATMENT

The theoretical framework used in the present paper has already been described by Sipe et al.[4] An example of fitting the SH intensity

patterns to calculation is also shown by Yamada and Kimura [2]. Here we only review the equations necessary for calculation. We take the *Z*-direction along the surface normal of the sample, and take the incident plane as the κ-*Z* plane. The *s*-axis is taken perpendicular to the incident plane (Fig. 2*a*) .

The *i*-th component of the bulk nonlinear optical polarization of a material with a nonlinear susceptibility $\chi^{(2)}_{ijk}$can be written as :

$$P^{(2)}_{NLi} = \chi^{(2)}_{ijk} E_j E_k \qquad (3.1)$$

Here, E_j and E_k on the right-hand side are the internal excitation field amplitudes and are related to the incident field amplitude $\vec{E}_0$ outside the medium by

$$\vec{E} = \mathbf{t}\vec{E}_0 \qquad (3.2)$$

Here, **t** is a transmission Fresnel factor defined by Sipe et al. [4]

To describe the bulk nonlinearity of GaAs we use the nonlinear susceptibility defined in the standard manner. [5] We denote the bulk nonlinear susceptibility of GaAs referred to the crystal axis frame (x, y, z) by $\chi^{(2)}_{i'j'k'}$(GaAs), referred to the substrate frame (X, Y, Z) by $\chi^{(2)}_{IJK}$(sub), and referred to the beam frame (κ, s, Z) by $\chi^{(2)}_{ijk}$(beam). The bulk nonlinear optical susceptibility $\chi^{(2)}_{IJK}$(sub) in the substrate frame of a vicinal GaAs(001) whose crystal axis is tilted by an angle θ toward the direction ξ indicated in Fig. 2*b* can be written as:

$$\chi^{(2)}_{IJK}(\text{sub}) = \chi^{(2)}_{i'j'k'}(\text{GaAs})\, R_{i'I}(\psi,\theta) R_{j'J}(\psi,\theta) R_{k'K}(\psi,\theta) \qquad (3.3)$$

$$R(\psi,\theta) = U_Z(\psi) U_X(-\theta) U_Z(-\psi) \qquad (3.4)$$

The angle between the direction ξ and the [100] axis is ψ. I, J, and K refer to the substrate frame, and i', j', and k' refer to the crystal axis frame. U_Y and U_Z are the unitary matrices that represent anti-clockwise rotation

of vectors about the Y and Z axes, respectively, in the substrate frame. When $\theta=0^o$ the coordinate (x, y, z) of the crystal axis frame coincides with the coordinate (X,Y,Z) of the substrate frame. The non-zero bulk nonlinear optical susceptibility $\chi^{(2)}_{i'j'k'}(GaAs)$ of the zinc-blende type crystal GaAs in the crystal axis coordinate can be written as [5]:

$$\chi^{(2)}_{xyz}(GaAs)=\chi^{(2)}_{xzy}(GaAs)=\chi^{(2)}_{yxz}(GaAs)=\chi^{(2)}_{yzx}(GaAs)=\chi^{(2)}_{zxy}(GaAs)=\chi^{(2)}_{zyx}(GaAs) \quad (3.5).$$

In our experiment the plane of incidence is rotated continuously with respect to the substrate frame (Fig. 2*a*). We define ϕ as the angle between the plane of incidence and the X-axis of the substrate frame. The nonlinear susceptibility $\chi^{(2)}_{ijk}(beam)$ in the beam frame can be written as:

$$\chi^{(2)}_{ijk}(beam) = \chi^{(2)}_{IJK}(sub)U_{Z,Ii}(-\phi)U_{Z,Jj}(-\phi)U_{Z,Kk}(-\phi) \quad (3.6)$$

According to Sipe et al [4], the *s*- and *p*-polarized electric fields outside the medium generated by a nonlinear polarization $\vec{P}^{(2)}_{NL}$ filling a half-space are,

$$E_s^{(2\omega)}= B_s(\hat{s}\cdot\vec{P}^{(2)}_{NL}) \quad (3.7)$$

$$E_p^{(2\omega)}= B_p(\hat{p}\cdot\vec{P}^{(2)}_{NL}) \quad (3.8)$$

Here, B_S and B_P are the nonlinear Fresnel factors, and the symbols $\hat{s}$ and $\hat{p}$ are the unit vectors of *s*- and *p*-polarization for the outgoing electric field in the medium. They were defined by Sipe et al. [4] $\vec{P}^{(2)}_{NL}$ is obtained from (3.1) and (3.6).

Now we turn to the surface nonlinearity. Following Guyot-Sionnest et al [6], we define the surface nonlinear susceptibility in the substrate frame as $\chi^{(2)}_{S,IJK}$. They define the surface nonlinear optical susceptibility tensor by first defining the bulk nonlinear susceptibility in a thin surface layer and then by integrating it over the surface layer as a function of depth. When some of the suffices of the susceptibility

include the coordinate Z, the integrand is divided by the dielectric function of the surface layer at the frequency of the corresponding photons. [6] Using this surface nonlinear susceptibility, we can write down the electric field amplitude of the surface SH wave in the beam frame coordinate as[7]:

$$E_{Ssout} = A_s\frac{4\pi i}{\lambda_\omega}[(\chi^{(2)}_{S,sZZ}f_s^2\varepsilon(\omega)^2+\chi^{(2)}_{S,sZK}f_sf_c\varepsilon(\omega)+\chi^{(2)}_{S,sKK}f_c^2)t_P^2E_{P0}^2 + (\chi^{(2)}_{S,sZs}f_s\varepsilon(\omega)+\chi^{(2)}_{S,sKs}f_c)t_Pt_SE_{P0}E_{S0} \quad +\chi^{(2)}_{S,sss}t_S^2E_{S0}^2] \tag{3.9}$$

$$E_{Spout} = A_p\frac{4\pi i}{\lambda_\omega}F_s\varepsilon(2\omega)[(\chi^{(2)}_{S,ZZZ}f_s^2\varepsilon(\omega)^2+\chi^{(2)}_{S,ZZK}f_sf_c\varepsilon(\omega)+\chi^{(2)}_{S,ZKK}f_c^2)t_P^2E_{P0}^2 + (\chi^{(2)}_{S,ZZs}f_s\varepsilon(\omega)+\chi^{(2)}_{S,ZKs}f_c)t_Pt_SE_{P0}E_{S0} \quad +\chi^{(2)}_{S,Zss}t_S^2E_{S0}^2] - A_p\frac{4\pi i}{\lambda_\omega}F_c[(\chi^{(2)}_{S,KZZ}f_s^2\varepsilon(\omega)^2+\chi^{(2)}_{S,KZK}f_sf_c\varepsilon(\omega)+\chi^{(2)}_{S,KKK}f_c^2)t_P^2E_{P0}^2 + (\chi^{(2)}_{S,KZs}f_s\varepsilon(\omega)+\chi^{(2)}_{S,KKs}f_c)t_Pt_SE_{P0}E_{S0} \quad +\chi^{(2)}_{S,Kss}t_S^2E_{S0}^2] \tag{3.10}$$

A_S, A_p, f_S, f_c, F_S, and F_c in the above equation are defined by Sipe et al. [4] $\varepsilon(\omega)$ and $\varepsilon(2\omega)$ are the dielectric constants of the medium at the fundamental and the second harmonic frequencies, respectively. λ_ω is the wavelength of the light at the fundamental frequency. Note that Eqs. (3.9) and (3.10) do not include the dielectric constants of the surface layer. The surface nonlinear susceptibility $\chi^{(2)}_{S,ijk}$ in the beam frame coordinate is related to the surface nonlinear susceptibility $\chi^{(2)}_{S,IJK}(sub)$ in the substrate frame by

$$\chi^{(2)}_{S,ijk} = \chi^{(2)}_{S,IJK}(sub)\,U_{Z,Ii}(\phi)U_{ZJj}(\phi)U_{Z,Kk}(\phi) \tag{3.11}$$

The total power of the SH field is given by,

$$I_\alpha = \left|E_\alpha^{(2\omega)} + E_{S\alpha out}\right|^2 \qquad (\alpha=p,s) \tag{3.12}$$

with $E_\alpha^{(2\omega)}$ and $E_{S\alpha out}$ defined in Eqs. (3.7) and (3.11). We do not consider the bulk electric quadrupolar polarization, following the earlier analysis by Yamada and Kimura. [2] In the analysis we will also use a

coordinate system (ξ, η, Z) defined in relation to the direction of the tilt of the crystal axes. (Fig. 2*b*)

4. RESULTS AND ANALYSIS

In Fig. 3 we show the polar plots of the SH intensity from a vicinal GaAs(001) as a function of the sample rotation angle. The incident angle of the exciting light is 45°. The large dots represent the data points obtained by the measurement, and the small dots represent the calculated results. The SH intensity is plotted along the radial direction and its relative scale is written in each figure. The calculation was carried out with adjustable parameters ψ, θ, and $\chi^{(2)}_{S,ijk}$(sub)'s. The inset at the center illustrates the direction of the atomic steps of the surface for ϕ=90°.

Based on the results by Yamada and Kimura [2] we made the adjustable parameters converge by the following three steps.

1) First, we looked at Fig. 3*d*. The surface nonlinear susceptibilities that should be effective in this Sin-Sout polarization configuration, are $\chi^{(2)}_{S,ijk}$(sub)'s(i,j,k=ξ,η). We found that none of these susceptibilities reproduces the data pattern. Thus they were assumed to be small. We could reproduce the experimental pattern when only the bulk nonlinear susceptibility of the tilted GaAs(001) substrate is considered. We looked for appropriate θ and ψ, and reproduced the peak heights of the SH intensity of the Sin-Sout (Fig. 3*d*)and Pin-Sout (Fig. 3*b*) configurations.

2) We looked for appropriate $\chi^{(2)}_{S,\xi\eta Z}$(sub) and $\chi^{(2)}_{S,\eta\xi Z}$(sub), and fitted the SH intensity of P-in-S-out (Fig. 3*b*) and S-in-P-out (Fig. 3*c*) configurations. During this process we needed to adjust the values of θ and ψ slightly.

3) We looked for appropriate $\chi^{(2)}_{S,ZZZ}(sub)$ and $\chi^{(2)}_{S,Z\eta Z}(sub)$ that fit the SH intensity pattern of P-in-P-out configuration (Fig. 3*a*).

The other components of $\chi^{(2)}_{S,ijk}(sub)$'s, except for the two components $\chi^{(2)}_{S,\xi Z\xi}(sub)$ and $\chi^{(2)}_{S,\eta Z\eta}(sub)$ mentioned later, do not reproduce the data pattern, and hence they were assumed to be small. After we reached step 3) we returned to step 1) and repeated the procedure. The parameters converged quickly. As shown in Fig. 3 we obtained fairly good calculated patterns. Not only the pattern shape but also the relative intensities among different polarization combinations were reproduced well. There was a large scatter in the data for S-in-P-out and S-in-S-out polarization combinations (Fig. 3*c* and *d*), because their absolute SH intensity was small. Thus we could not obtain a complete fit to every data point in these polarization configurations.

We notice here that the ϕ dependence for *s*-incidence is very sensitive to the tilt angle of the crystal axis. Especially, the SH intensity of S-in-S-out configuration is a direct measure of the tilt angle, because the SH intensity of this configuration is zero, if the tilt angle θ is zero. So the measurement in this polarization configuration is very important in determining the tilt angle of the wafer.

We obtained the following parameters ψ, θ and non-zero $\chi^{(2)}_{S,ijk}(sub)$ for the present sample:

$$\psi = 90 \pm 3 \ ^{o}$$
$$\theta = 2.1 \pm 0.2 \ ^{o}$$

(4.1)

$$\chi^{(2)}_{S,ZZZ}(sub) = -0.039\ i\ \ \chi^{(2)}_{xyz}(GaAs)\ [esu\cdot Å]$$
$$\chi^{(2)}_{S,\xi\eta Z}(sub) = 0.12\ i\ \ \chi^{(2)}_{xyz}(GaAs)\ [esu\cdot Å]$$
$$\chi^{(2)}_{S,Z\eta Z}(sub) = -0.079\ i\ \ \chi^{(2)}_{xyz}(GaAs)\ [esu\cdot Å]$$

(4.2).

The component $\chi^{(2)}_{S,\eta\xi Z}$(sub) turned out to be small. The unit [esu Å] indicates that the surface nonlinear susceptibility $\chi^{(2)}_{S,ijk}$ has a unit of bulk second-order nonlinear susceptibility multiplied by a unit of length. Thus [esu Å] is equal to 10^{-8} [esu]. The bulk nonlinear susceptibility of GaAs $\chi^{(2)}_{xyz}$(GaAs) is $(140\pm10) \times 10^{-8}$ in the unit of [esu]. This value was obtained by extrapolation of the dispersion of the bulk nonlinear susceptibility obtained by Lotem and Yacoby. [8]

As pointed out by Yamada and Kimura [1,2], the $\chi^{(2)}_{S,ijk}$(sub)'s cannot generally be determined uniquely. If we adopt as alternative parameters,

$$\chi^{(2)}_{S,\xi Z\xi}(\text{sub}) = \chi^{(2)}_{S,\eta Z\eta}(\text{sub}) = 0.30\, i\ \chi^{(2)}_{xyz}(\text{GaAs})\ [\text{esu}\cdot\text{Å}] \qquad (4.3)$$

instead of $\chi^{(2)}_{S,ZZZ}$(sub) in (4.2), we obtain exactly the same patterns. However, there are no other alternatives than (4.2) and (4.3) as far as we can see in our manual scan of the parameter space. Because we have the experimental data for all four polarization combinations, there is less ambiguity in our fitting than in earlier authors' results [1-3]. The choice between parameter set (4.2) and the parameter set (4.2) with $\chi^{(2)}_{S,ZZZ}$(sub) replaced by (4.3) can be made when the dependence of the SH intensities on the incident angle of excitation is known. This is a future problem. The tilt parameters ψ and θ were not affected by our choice of $\chi^{(2)}_{S,ijk}$(sub)'s; i. e. (4.2) or (4.3).

We note here that without the surface nonlinearity the pattern for *p*-excitation and *s*-output in Fig. 3(b) is modified. This modification corresponds to the tilt angle of the axis of about 0.2^{o}. Thus, if the surface nonlinearity is not considered as in ref. 3, an error in the estimation of the tilt angle of 0.2^{o} will arise.

The tilt parameters obtained by X-ray analysis of the present sample are

$$\psi = 90 \pm 10^{\circ}$$
$$\theta = 2.0 \pm 0.3^{\circ} \qquad (4.4)$$

The parameters in (4.1) obtained by SHG and those in (4.4) obtained by X-ray diffraction agree very well. Thus, we see that the SHG method is adequate for the determination of the tilt angle of the GaAs(001) wafer. The method by SHG can be superior to that by X-ray diffraction in several ways. The accuracy in measuring θ and ψ depends on the degree how ideally plane the probe beam is. Optical beams generated by ordinary pulse lasers are usually much better plane waves than the X-ray beams from ordinary X-ray sources. Thus, we can expect that a method that uses lasers would give a higher ultimate accuracy in determining the tilt parameters than a method based on the X-ray. Also, laser light is easier to handle than the X-ray and has less health hazard than the X-ray. A further check of the potential use of this method is a future problem.

We also point out that the present analysis can be used as a method for distinguishing [110] and $[1\bar{1}0]$ directions of GaAs(001) wafers. In the *p*-incidence and *p*-output polarization combination (Fig. 3*a*), the peak at ϕ=135° is higher than that at ϕ=45°, and the peak at ϕ=315° is higher than that at ϕ=225°. If we only consider the bulk contribution, the pattern in Fig. 3*a* should show a symmetry between the upper and lower halves. This is because the atomic arrangement under the surface of the present sample is symmetric with respect to (100) plane if we do not distinguish between Ga and As atoms. A similar behavior of SH peak intensities was always observed when we observed SH patterns from other samples. As an example we show the result for a GaAs(001) wafer without a tilt in Fig. 4. The calculation shows that if there is no surface contribution the pattern has a four-fold symmetry. The lowered symmetry seen in Fig. 4 is not due to residual misorientation of the

substrate. Calculations show that a tilt of the axes of the substrate does not reduce the SH intensity at two peaks on opposite sides in the pattern, i. e. at ϕ=45^{o} and 225^{o}, simultaneously. The change of the pattern arises from the interference between the isotropic surface SHG and the bulk SHG. The signs of the nonlinear susceptibility components for the exciting electric fields in the (110) and $(1\bar{1}0)$ planes are opposite. This is because the bulk Ga-As-Ga-As- chain along [110] has Ga atoms higher than As atoms and Ga-As-Ga-As- chain along $(1\bar{1}0)$ has As atoms higher than Ga atoms(Fig. 5). This phase difference of 180^{o} between the electronic wavefucntions of the two bulk chains leads to the difference in the interference between the bulk and surface SHG and to the change of the SH peak intensities. Thus, to observe this interference is equivalent to see the phase of the electronic wavefunction of the Ga-As chains. A similar trend in the SH intensity pattern is also seen for clean GaAs(001) surfaces in UHV. [1]

A non-destructive method for distinguishing between the [110] and $[1\bar{1}0]$ directions of GaAs(001) wafers by SHG should be useful for practical purposes. In our daily handling of GaAs wafers there are occasions when the information on the [110] and $[1\bar{1}0]$ directions is accidentally lost by a careless cleavage. In such cases the SHG method is useful in recovering the information. X-ray analysis cannot obtain this information.

In conclusion, we have observed and analyzed the SH intensity patterns of four combinations of the *p*- and *s*-incident and output light polarizations on GaAs(001) wafer, that is crystallographically tilted towards the [010] direction. We have obtained the tilt parameters and the surface nonlinear optical susceptibility tensor of this wafer. The tilt of the crystal axes determined from the SHG data agrees well with that obtained by a X-ray diffraction measurement. We propose that the

SHG method gives another means for measuring the tilt parameters of GaAs substrate. We have also shown that the [110] and [$1\bar{1}0$] directions can be distinguished through the analysis of *p*-incident and *p*-output SH intensity patterns.

ACKNOWLEDGMENT

We thank Y. Akama of Tohoku University for his technical assistance and advice. We also thank Prof. Y. R. Shen of University of California, Berkeley for valuable discussions and advice. This work was supported in part by a Grant-in-Aid for Scientific Research from the Ministry of Education, Science, Sports, and Culture.

REFERENCE

*Present Address: Kokusai Electric Co., LTD., 2-1 Yasuuchi, Yatsuo-machi, Nei-gun, Toyama-ken 939-23

[1] C. Yamada and T. Kimura, Phys. Rev. Lett. **70**, 2344 (1993).

[2] C. Yamada and T. Kimura, Phys. Rev. **49**, 14372 (1994).

[3] D. J. Bottomley, G. Lüpke, J. G. Mihaychuk, and H. M. van Driel, J. Appl. Phys. 74, 6072 (1993).

[4] J. E. Sipe, D. J. Moss, and H. M. van Driel, Phys. Rev. **35**, 1129 (1987).

[5] Y. R. Shen, *The principles of Nonlinear Optics* (Wiley, New York, 1984)

[6] P. Guyot-Sionnest, W. Chen, and Y. R. Shen, Phys. Rev. **33**, 8254 (1986).

[7] T. Yamauchi, G. Mizutani, S. Ushioda, to be published.

[8] H. Lotem and Y. Yacoby, Phys. Rev. **B10**, 3402 (1974).

FIGURE CAPTIONS

Fig. 1 Block diagram of the experimental setup.

Fig. 2 (a) The beam frame coordinate (κ, s, Z) and the substrate coordinate (X, Y, Z). The plane of incidence is the shadowed parallelogram. The angle between this plane and the X axis of the substrate coordinate is ϕ. (b) The definition of the tilt angle of the crystal axis. The size of the atomic steps are exaggerated in the figure. The crystal axis is tilted by an angle θ towards the direction denoted by ξ. The angle between direction ξ and the [100] axis is denoted by ψ. (X, Y, Z) is the substrate frame coordinate and (ξ, η, Z) is the coordinate defined relative to the direction of the tilt. The axis Z is common to the two frames. ξ is taken along the direction of the tilt.

Fig. 3 The SH intensity patterns of a vicinal GaAs(001) wafer with crystal axes tilted by 2.0 degrees toward the [010] direction. The incident and the output polarizations are written in the figure. The larger solid dots represent the experimental data and the smaller solid dots represent the calculated results. The central inset illustrates the direction of the atomic steps for ϕ=90^{o}. The incident angle is 45^{o} from the surface normal.

Fig. 4 The SH intensity patterns of GaAs(001) wafer without a tilt of the crystal axis. The incident angle is 45^{o}. The incident and output light polarizations are both *p*.

Fig. 5 The crystal structure of bulk GaAs. The chains Ga-As-Ga-As- .. along the [110] and [$1\bar{1}0$] directions are indicated with thick lines.

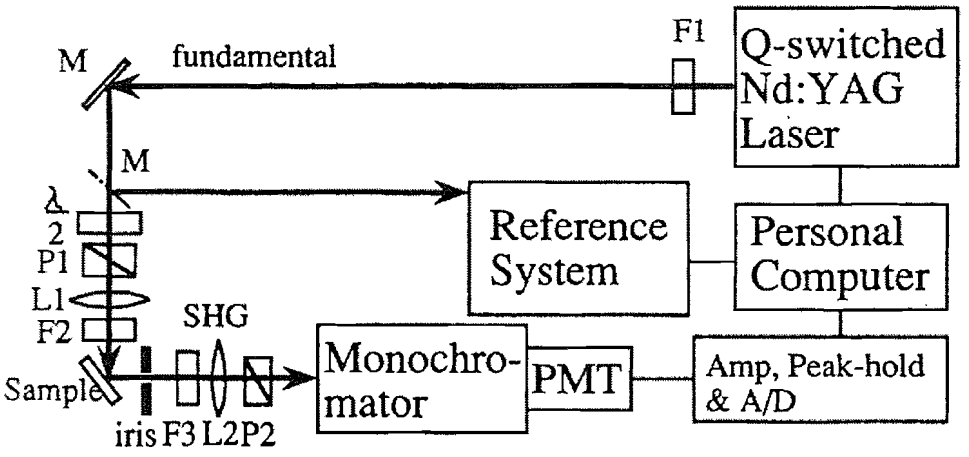

F1,F2: visible-cut filter
F3: IR-cut filter
M: mirror
Pi: polarizer
Li: lenses
PMT: photomultiplier tube

Figure 1 Takebayashi et al

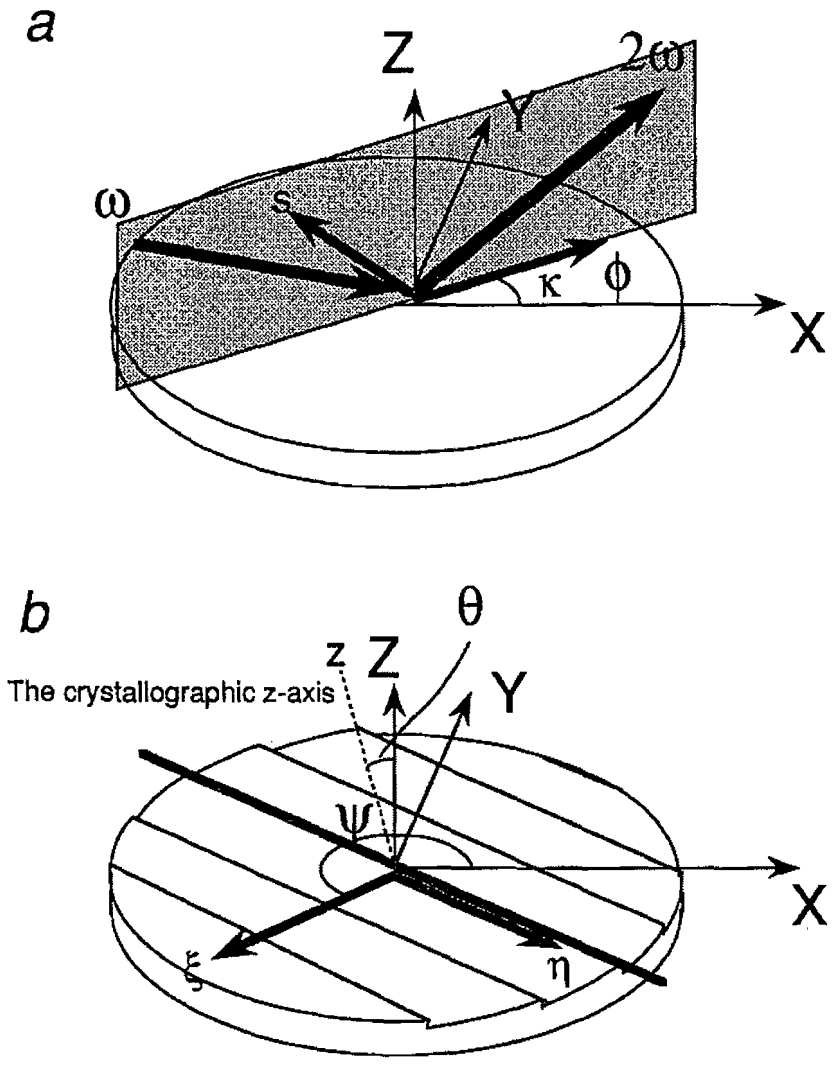

Figure 2 Takebayashi et al

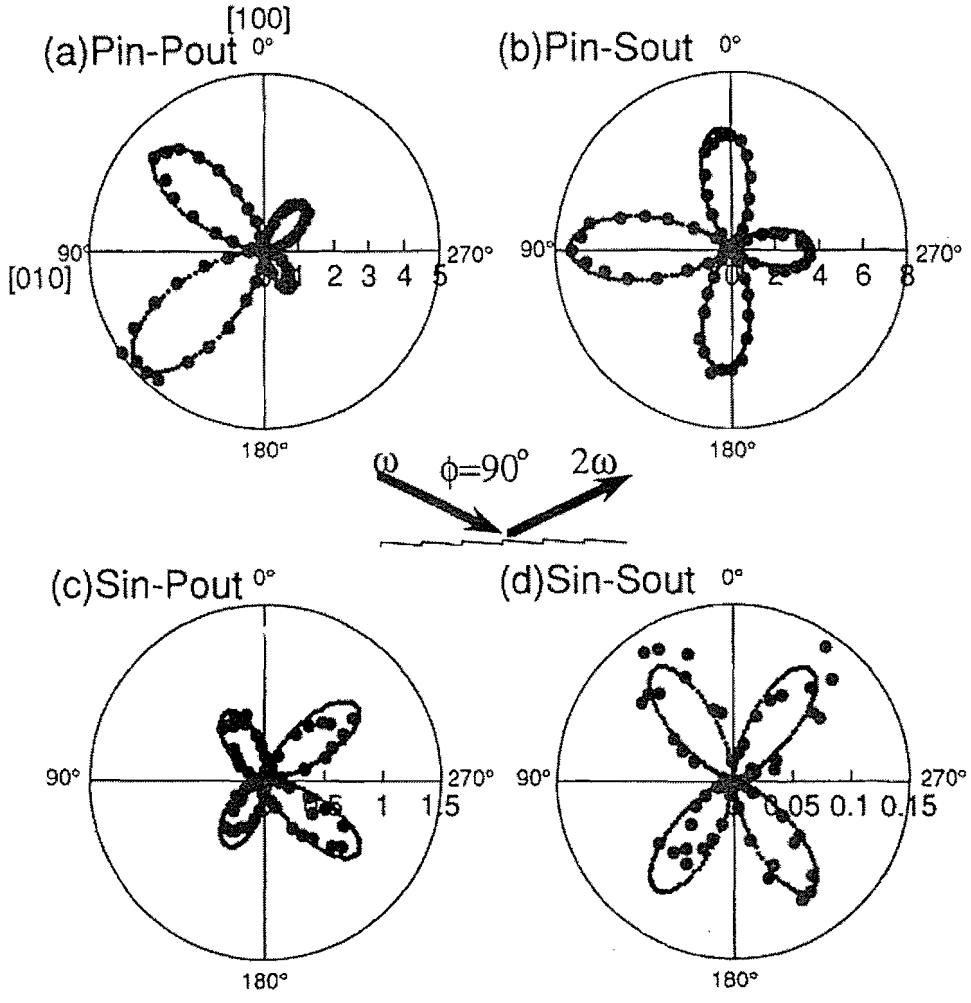

Figure 3 Takebayashi et al

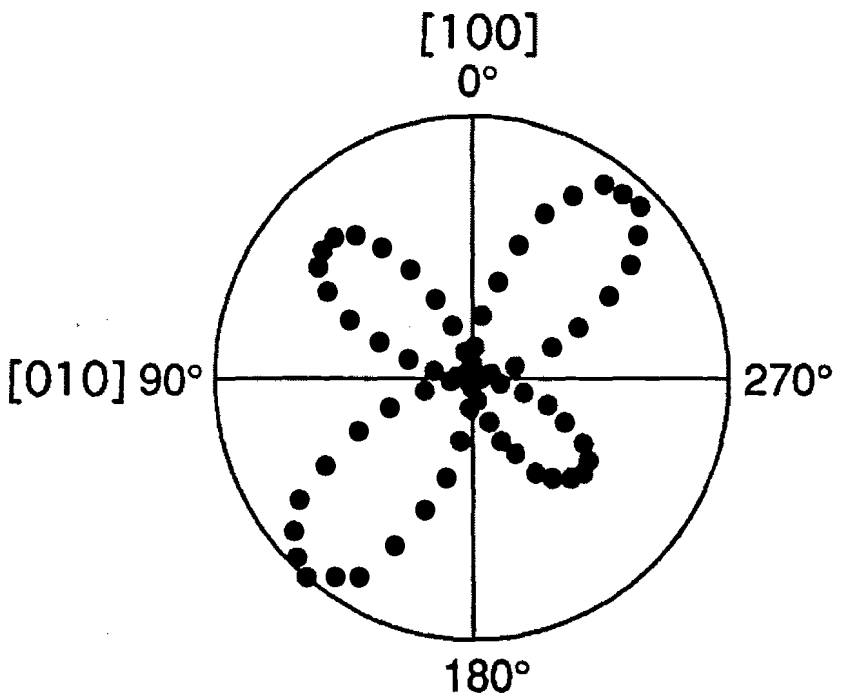

Figure 4 Takebayashi et al

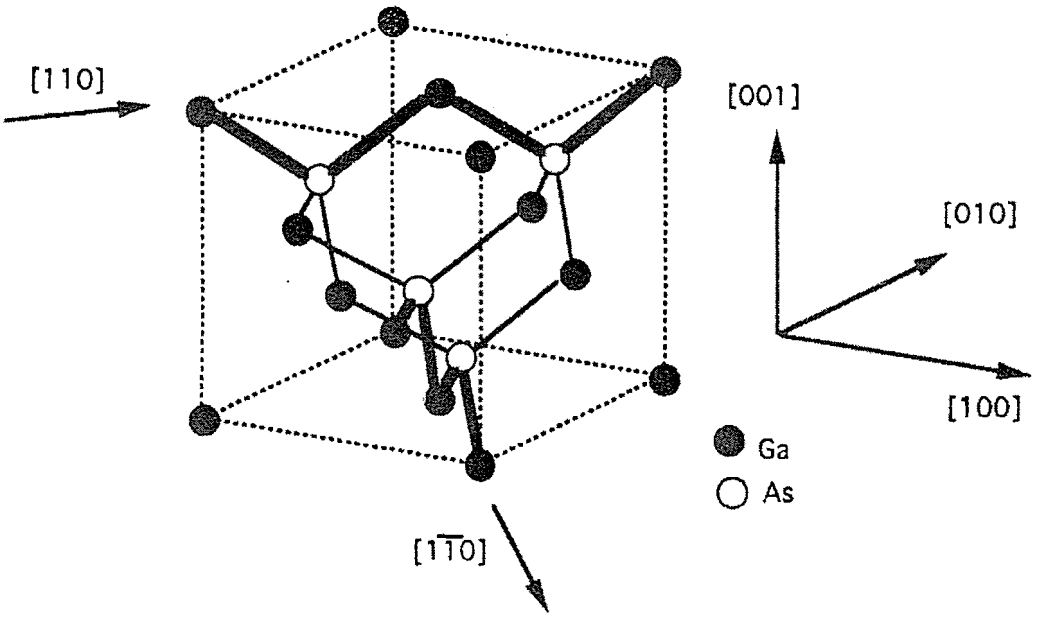

Figure 5 Takebayashi et al